AIP Physics of Plasmas

# Refraction of the ordinary wave near the electron cyclotron fundamental

D. C. McDonald, R. A. Cairns, C. N. Lashmore-Davies, and G. Le Clair

Citation: Phys. Plasmas 5, 883 (1998); doi: 10.1063/1.872655
View online: http://dx.doi.org/10.1063/1.872655
View Table of Contents: http://pop.aip.org/resource/1/PHPAEN/v5/i4
Published by the American Institute of Physics.

PHYSICS OF PLASMAS VOLUME 5, NUMBER 4 APRIL 1998

# Refraction of the ordinary wave near the electron cyclotron fundamental

D. C. McDonald[a]
*Department of Physics and Astronomy, University of Glasgow, Glasgow G12 8QQ, United Kingdom*

R. A. Cairns
*School of Mathematical and Computational Sciences, University of St. Andrews, St. Andrews, Fife KY16 9SS, United Kingdom*

C. N. Lashmore-Davies
*UKAEA Fusion, Culham Science Centre, Abingdon, Oxfordshire, OX14 3DB, United Kingdom*

G. Le Clair
*Centre Canadien de Fusion Magnetique, Varennes, Québec S3X 1S1, Canada*

(Received 29 September 1997; accepted 16 January 1996)

Detailed ray tracing, of wave propagation in a plasma near electron cyclotron resonances, suggests that refraction can lead to reduced absorption, in some cases. By studying the full wave equation for the ordinary wave near the fundamental, in a slab model, it is shown that such refraction does indeed reduce absorption, for this particular case, but that wave energy tunnelling can significantly modify the result. © *1998 American Institute of Physics.* [S1070-664X(98)04504-2]

## I. INTRODUCTION

The study of electron cyclotron resonant heating requires a description of wave propagation through a plasma, for which Wentzel–Kramers–Brillouin (WKB) ray tracing[1] is a routine technique. Much ray tracing has been done using the cold plasma dispersion relation to calculate the path of the rays. However, recent work[2–6] has shown that warm plasma contributions to the dispersion relation, close to the resonance, can result in significant refraction effects. In certain cases, these can prevent wave energy reaching a resonance, and so eliminate absorption. Ray tracing near a resonance, though, should be treated with caution, as the WKB conditions of validity often break down. Here, we look at a full wave calculation for a wave near an electron cyclotron resonance, and compare the results with those of ray tracing. Earlier workers[7–10] studied full wave equations for wave propagation in magnetic field gradients, but did not consider a component of the wave vector in the direction perpendicular to both the field and its gradient (which we shall later take as the $y$-direction). The inclusion of this wave vector component will allow us to study the wave refraction effects seen in Refs. 2–6.

Specifically, we shall examine the ordinary mode propagating in a warm plasma, perpendicularly to an applied magnetic field, approaching the fundamental resonance from the low field side. We consider a slab model, with inhomogeneity in the $x$-direction and the magnetic field lying in the $z$-direction. The wave then propagates in the $x$-$y$ plane and resonates with the fundamental ($\omega=\omega_{ce}$) at $x=0$. About the resonance we may Taylor expand the field as

$$B(x)=B(0)\left(1-\frac{x}{L}\right)+O(x^2). \tag{1}$$

The plasma is assumed to be weakly relativistic ($\mu=m_e c^2/\kappa T_e \gg 1$) and so has an absorption width ($\delta=L/\mu$) that is much smaller than the scale length of the macroscopic plasma parameters, but may be comparable to the wavelength of the propagating wave.

## II. WAVE EQUATIONS

We wish to compare a full wave equation treatment of our system with that of ray tracing—where the path of the wave is calculated and the absorption is integrated along this path. We shall distinguish between ray tracing following rays given by the cold plasma dispersion relation (cold plasma ray tracing) and rays given by the weakly relativistic dispersion relation (hot plasma ray tracing).

Our derivation of the full wave equation follows Ref. 10. The resulting equation is

$$\frac{d}{dx}\left[\{1+f(x)\}\frac{dE_z}{dx}\right]+\left[-\{1+f(x)\}k_y^2+\frac{df}{dx}k_y+\frac{\omega^2-\omega_{pe}^2}{c^2}\right]\times E_z=0, \tag{2}$$

where

$$f(x)=\frac{1}{2}\frac{\omega_{pe}^2}{\omega_{ce}^2}F_{7/2}\left(\mu\frac{\omega-\omega_{ce}}{\omega}\right).$$

The function denoted by $F_{7/2}$ is a Dnestrovskii function.[11–13]

We now turn to ray tracing. Cold plasma theory gives us the ordinary mode dispersion relation $N_x^2+N_y^2=N_{\perp cold}^2=1-\alpha$, where $\alpha=\omega_{pe}^2/\omega^2$. Outside the resonance region, $|x|\gg\delta$, this describes very accurately the path of a ray, and so we may use it to describe the trajectory from its launch until it reaches the resonance region. Provided $\alpha<1$ (that is, the density is below the cut off density) everywhere, the wave will propagate towards the resonance on a ray de-

[a]Electronic mail: darren@astro.gla.ac.uk

termined by cold plasma theory and will be incident on the resonance, from the low field side, at an angle $\theta$ to the $x$-direction. (This incident angle will, in general, differ from the angle of launch due to wave refraction as the wave travels towards the resonance region.) Local to the resonance, where we may approximate density, and hence $\alpha$, as constant, cold plasma theory would predict that the rays would propagate through the region in straight lines. However, in this region warm plasma effects are significant.

The hot plasma dispersion relation can be calculated by a WKB solution of Eq. (2), namely,

$$N_\perp^2 = N_x^2 + N_y^2 = \frac{1-\alpha}{1+f}. \tag{3}$$

Far from resonance ($f \to 0$) we have the cold plasma limit with $N_\perp^2 = N_{\perp cold}^2$. We are considering, as stated above, the trajectory of a wave incident from the low field side where, as there is no absorption, the $F$ function is real. As the wave moves towards the resonance $N_\perp^2$, and consequently $N_x^2$, will decrease monotonically. If $N_y^2$ is above the threshold value of $N_\perp^2$ at the resonance, Fig. 1(a), $N_x^2$ will go to zero at some point ($x = x_{cutoff}$) and the wave will be refracted away before reaching the resonance [Fig. 1(b)]. This would occur for angles of incidence above a critical angle ($\theta_{crit}$) given by

$$\mathrm{cosec}^2\ \theta_{crit} = 1 + \frac{\alpha}{5}, \tag{4}$$

where we have noted[13] that at $x=0$, $F_{7/2} = 2/5$. According to hot plasma ray tracing then, rays incident with $\theta \geqslant \theta_{crit}$ will experience no absorption.

To study the full wave equation in the vicinity of the fundamental, we use the local magnetic field approximation, Eq. (1), and rescale $x$ to the cold plasma inverse wave number, to get

$$\frac{d}{dx'}\left[\{1+f'\}\frac{dE_z}{dx'}\right] + \left[1 - f'\tan^2\ \theta + \frac{df'}{dx'}\tan\ \theta\right]E_z = 0, \tag{5}$$

where

$$f(x') = \frac{\alpha}{2}F_{7/2}\left(\frac{x'}{\delta'\ \cos\ \theta}\right), \quad \delta' = \frac{\omega L}{\mu c}(1-\alpha)^{1/2},$$

and

$$x' = x\frac{\omega}{c}(1-\alpha)^{1/2}\cos\ \theta.$$

This equation can then be integrated numerically, with boundary conditions for low field incidence, for various values of the parameters $\alpha$ and $\delta'$, and different angles of incidence, $\theta$.

Figures 2(a)–2(c) show plots of transmission, reflection and absorption, against the angle of incidence, for $\alpha = 0.5$ and three different values of $\delta'$, corresponding to plasmas that have small, intermediate and large optical thicknesses, respectively. In each case, cold plasma ray tracing predicts[1] a transmitted wave with refraction, $R=0$, transmission, $T = \exp(-\tau)$ and absorption, $A = 1 - T$, where $\tau$ is the optical thickness given by

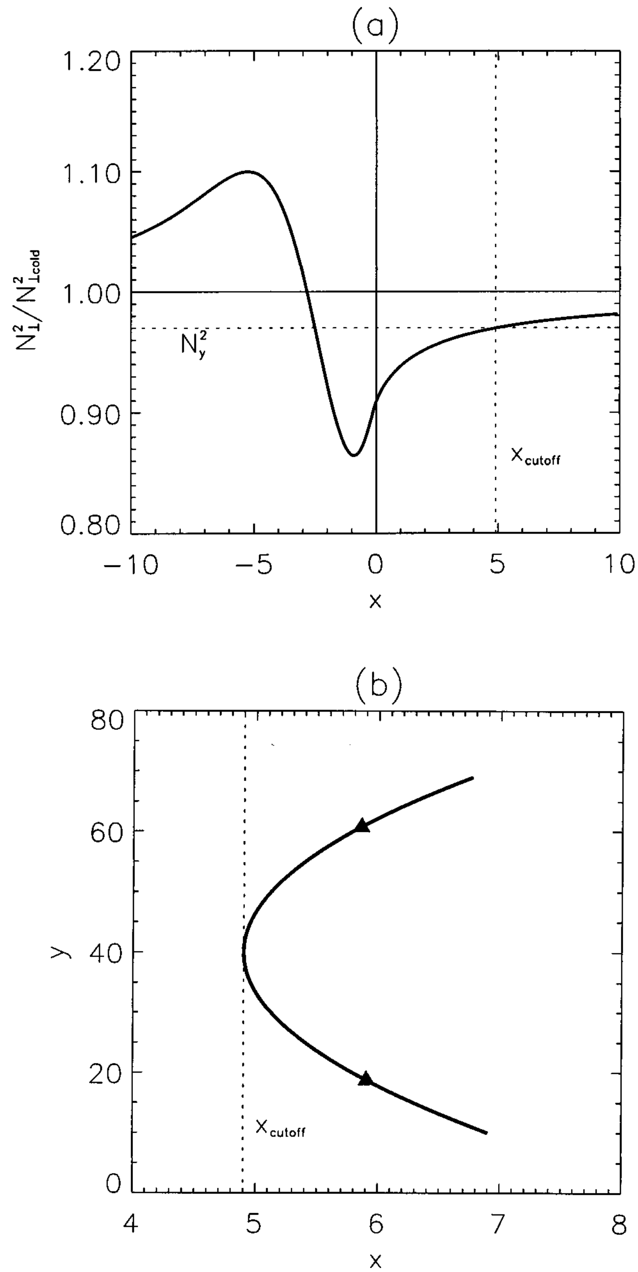


FIG. 1. Refraction of the wave by the $x$ cutoff for $\alpha = 0.5$. (a) Refractive index; (b) ray path.

$$\tau = \frac{\pi\delta'}{4}\sec\ \theta. \tag{6}$$

Hot plasma ray tracing would agree with this for $\theta < \theta_{crit}$, but then would predict total reflection thereafter.

Despite the inability of cold plasma ray tracing to describe the reflection seen in the hot plasma theory, and hence give an accurate measure of absorption in all cases, it does give a good description of the transmission in all parameter ranges. This is in agreement with previous work,[4,7–10] for $\theta = 0$, and is illustrated in Fig. 3 for the case $\alpha = 0.5$ and $\delta' = 0.5$.

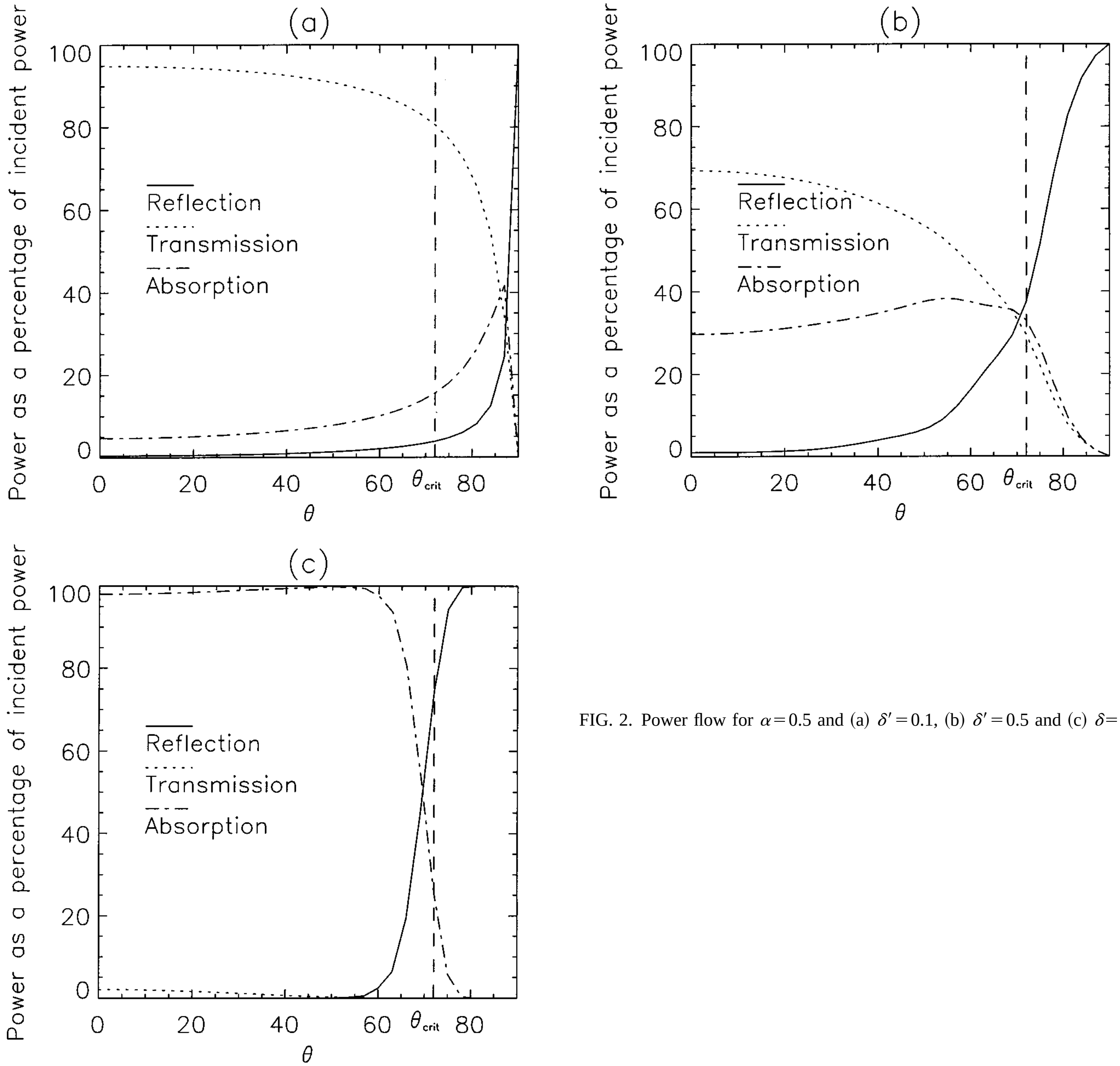


FIG. 2. Power flow for $\alpha=0.5$ and (a) $\delta'=0.1$, (b) $\delta'=0.5$ and (c) $\delta=5$.

The full wave picture is more complicated than that given by ray tracing. Wave energy tunnelling through the evanescent region is the extra ingredient introduced by the full wave analysis and leads to finite transmission and absorption for $\theta > \theta_{crit}$. The amount of tunnelling is crucially dependent on the value of $\delta'$.

For small $\delta'$ [Fig. 2(a)] the plasma is optically thin and hence there is strong transmission below $\theta_{crit}$, in good agreement with ray tracing. However, due to tunnelling, strong transmission continues even above $\theta_{crit}$, and so we see a marked difference from hot plasma ray tracing.

For intermediate $\delta'$ [Fig. 2(b)] the picture is even more complicated. Full wave effects mean that we now see reflection for $\theta < \theta_{crit}$ and, once more, there is significant transmission, due to tunnelling, for $\theta > \theta_{crit}$. Most significantly, there is appreciable absorption (over 30%) at $\theta_{crit}$, where hot plasma ray tracing predicts complete reflection.

Finally, large $\delta'$ [Fig. 2(c)] results are much more in agreement with hot plasma ray tracing. Absorption is generally strong below $\theta_{crit}$ and then negligible above it. This is due to the large tunnelling region. However, it should be noted that here full wave effects lead to large reflection for angles below $\theta_{crit}$.

The key parameter, in describing tunnelling, is $\delta' \cos\theta = k_{xcold}\delta$, the ratio of the absorption width to the inverse wave number of the cold plasma wave in the $x$ direction (which can be thought of as the width of the resonance region in terms of wavelengths of the incoming wave). This is illustrated in Figs. 4(a)–4(c): contour plots of reflection, transmission and absorption, respectively, against $\alpha$ and $\delta' \cos\theta$ for $\theta = \theta_{crit}$, where hot plasma ray tracing predicts complete reflection.

For values of $\delta' \cos\theta$ well above unity, the tunnelling region is much larger than a wavelength, and so reflection is high, with little wave energy reaching the absorption region.

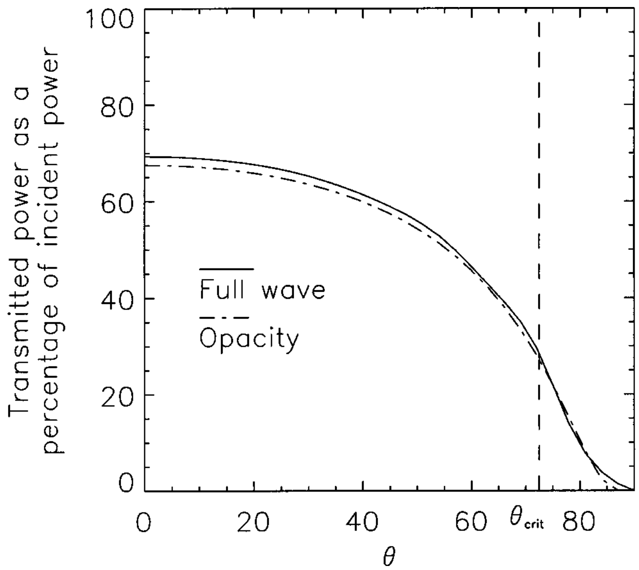


FIG. 3. Comparison of transmission coefficients, from full wave and opacity calculations, for $\alpha=0.5$ and $\delta'=0.5$.

This is in good agreement with hot plasma ray tracing. For values of $\delta'\cos\theta$ well below unity, however, the tunnelling region is smaller than a wavelength, so reflection becomes small and most wave energy reaches the absorption region. This is consistent with cold plasma ray tracing. At the same time, though, the absorption width is also much less than a wavelength and so most of the wave energy reaching the resonance passes through as transmitted power. This means that the region for which maximum absorption takes place results from a trade off between these two extremes with $\delta'\cos\theta_{crit}\approx 0.4$ for which the absorption is around 40%. Consequently, it is correct to say that refraction effects prevent absorption of most of the rf power for $\theta\geqslant\theta_{crit}$.

To see the trajectory of a wave, we must study a group of waves. This is done by taking the superposition of the plane wave solutions of Eq. (2), $E(x;k_y,\omega)$, with a Gaussian amplitude distribution about $k_{y0}$ of width $\delta k_y$,

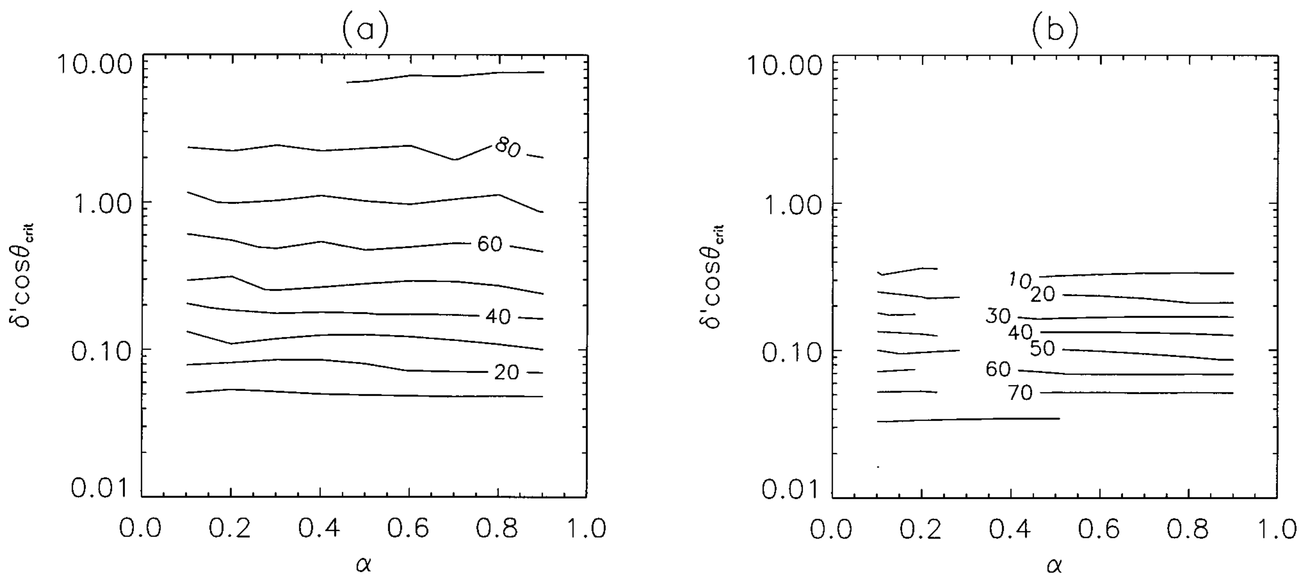


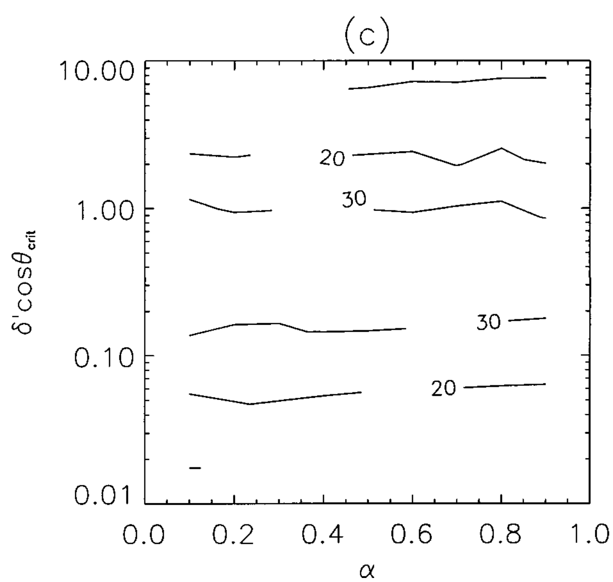


FIG. 4. Contour plots showing (a) reflection, (b) transmission and (c) absorption of wave energy from the fundamental resonance, calculated through integration of the full wave equation, Eq. (5).

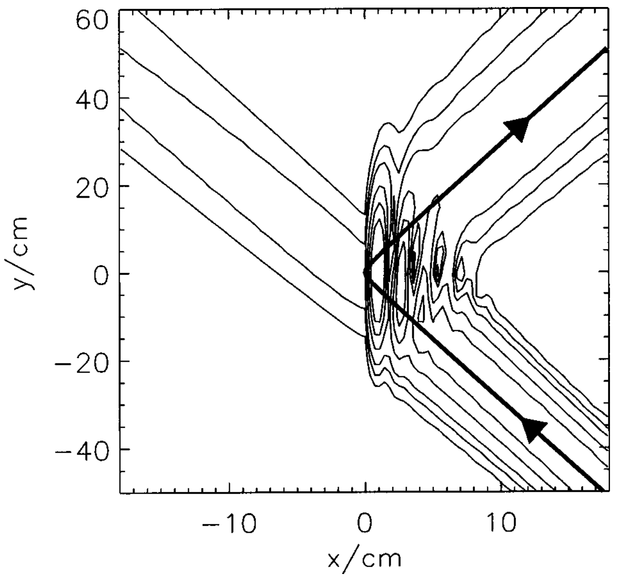


FIG. 5. Contour plot of a finite width wave for $n_{e0}=3.0\times10^{19}\ \mathrm{m}^{-3}$, $B_0=2.0$ T, $R_0=83$ cm, $T_e=0.5$ keV with angle of launch $\theta=70°$ and spread of 2°. The bold line denotes the trajectory of the hot plasma ray.

$$E_{group}(x;k_{y0},\delta k_y,\omega)=\int_{-\infty}^{\infty}dk_yE(x;k_y,\omega)\times\exp\left[-\frac{(k_y-k_{y0})^2}{\delta k_y^2}\right]. \quad (7)$$

A typical such wave group, using parameters typical of the Tokamak de Varennes,[14] is shown in Fig. 5, with the hot plasma ray superimposed on top of it. The parameters taken correspond to $\alpha=0.773$ and $\delta'=0.455$, and an angle of incidence higher than $\theta_{crit}$.

The wave group is incident from the bottom right and approaches the resonance region, where we see a complicated structure due to the superposition of incident and reflected waves. We then see the wave split into a transmitted part, that propagates to the left, and a refracted part propagating to the right. The total reflected power is 50.9%, the total transmitted power is 19.7% and the total absorption is 29.4%.

We see that the path of the group envelope agrees closely with that of hot plasma ray tracing, but we also note that there is now significant transmitted power. As we have a bundle of waves, we would expect some transmission to be predicted by hot plasma ray tracing—corresponding to the small number of rays with $\theta<\theta_{crit}=68.5°$—but this would be small and antisymmetric, in contrast to the symmetric 19.7% transmission seen here. Thus, hot plasma ray tracing describes the trajectory of the refracted wave group well, but does not describe the wave splitting.

## III. DISCUSSION

Our analysis, of the full wave calculation for the ordinary wave in a slab model, has allowed us to study the correspondence between ray tracing and the more exact theory. The degree of correspondence has been shown to be dependent on a tunnelling parameter, $k_{xcold}\delta$, the ratio of the absorption width to the inverse wave number in the direction of the field gradient. We have seen that for $k_{xcold}\delta\gg1$, refraction prevents absorption, in agreement with hot plasma ray tracing. However, for $k_{xcold}\delta\ll1$, wave tunnelling results in a reduction of this refraction effect and most wave energy does indeed reach the resonance layer, in agreement with cold plasma ray tracing, although for such parameters absorption will be small. For $k_{xcold}\delta\sim1$ we will see absorption, together with a combination of both reflection and transmission (wave splitting), which can only be described by a full wave calculation.

If we look at parameters typical of the Compact Assembly Tokamak (COMPASS-D[15]):—major radius ($R_0$) 0.557 cm, central magnetic field ($B_0$) 2.14 T, central electron temperature ($T_e$) 0.6 keV (i.e., at the start of the auxiliary heating phase) and central electron density ($n_{e0}$) $3.1\times10^{19}\ \mathrm{m}^{-3}$—we will have, at $\theta=\theta_{crit}$, $k_{xcold}\delta=0.16$. For $T_e=5$ keV (at the end of plasma heating) we would have $k_{xcold}\delta=1.31$ at $\theta=\theta_{crit}$. The behavior at the beginning of the heating phase will differ dramatically from the complete reflection predicted by hot plasma ray tracing. Reflection will in fact be around 30% and transmission around 40%. Towards the end of the heating, reflection does become more significant (up to around 70%) but we still see a noticeable departure from the hot plasma ray tracing. It should be noted, however, that the smallness of $k_{xcold}\delta$ will result in a low absorption coefficient and, as a result, second harmonic extra-ordinary mode heating is favoured on such experiments. The second harmonic extra-ordinary mode has a significantly shorter wavelength which will result in values for $k_{xcold}\delta$ above unity, suggesting better agreement with hot plasma ray tracing. However, we have not dealt with this case specifically in this paper and so further work remains to be done to demonstrate this explicitly.

For typical parameters of the Joint European Torus (JET[16]):—$R_0=3$ m, $B_0=2.7$ T, $T_e=0.5$ keV and $n_{e0}=5.0\times10^{19}\ \mathrm{m}^{-3}$, at $\theta=\theta_{crit}$, we would have $k_{xcold}\delta=0.89$, rising to $k_{xcold}\delta=8.9$ for $T_e=5$ keV. Hence, if electron cyclotron resonant heating at the fundamental were employed on a tokamak of this size or larger, we would expect hot plasma ray tracing to describe wave propagation for all but the lower end of the heating phase, and so we would see large amounts of refraction away from the resonance region for angles of incidence above $\theta_{crit}$.

## ACKNOWLEDGMENTS

The authors wish to thank Y. R. Lin-Liu, for useful discussions, and the anonymous referee who made a number of useful and constructive suggestions.

This work was jointly funded by the UK Engineering and Physical Sciences Research Council, Grant GR/K 58937. Support was also provided by the UK Department of Trade and Industry and Euratom.

[1] M. Bornatici, R. Cano, O. De Barbieri, and F. Engelmann, Nucl. Fusion **23**, 1153 (1983).
[2] S. Pešić and A. Stojić, J. Phys. Soc. Jpn. **62**, 2359 (1993).

[3] S. Pešić, Europhys. Lett. **35**, 349 (1996).
[4] E. Westerhof, Plasma Phys. Controlled Fusion **39**, 1015 (1997).
[5] G. Le Clair, I. P. Shkarofsky, Y. Demers, and J-F. Mercier, ''Electron cyclotron ray tracing,'' *Proceedings of the 12th AIP Topical Conference on Radio Frequency Power in Plasmas*, Savannah, 1997, Woodbury, New York (American Institute of Physics, Woodbury, 1997), p. 219.
[6] Y. R. Lin-Liu, T. C. Luce, S. C. Chiu, and R. L. Miller, ''Modelling of 110 GHz electron cyclotron wave propagation and absorption on DIII-D,'' Ref. 5, p. 195.
[7] K. Imre and H. Weitzner, Phys. Fluids **28**, 3572 (1985).
[8] C. Maroli, V. Petrillo, G. Lampis, and F. Engelmann, Plasma Phys. Controlled Fusion **28**, 615 (1986).
[9] V. Petrillo, G. Lampis, and C. Maroli, Plasma Phys. Controlled Fusion **29**, 877 (1987).
[10] D. C. McDonald, R. A. Cairns, and C. N. Lashmore-Davies, Phys. Plasmas **1**, 842 (1994).
[11] Yu. N. Dnestrovskii, D. P. Kostomarov, and N. V. Skrydlov, Sov. Phys. **8**, 691 (1964).
[12] I. P. Shkarofsky, Phys. Fluids **9**, 570 (1966).
[13] P. A. Robinson, J. Math. Phys. **27**, 1206 (1986).
[14] R. Decoste, J.-L. Lachambre, G. Abel, A. Boileau, C. Boucher, A. Cote, T. Fall, J.-L. Gauvreau, B. C. Gregory, E. Haddad, C. Janicki, C. Liu-Hinz, H. H. Mai, F. Martin, D. Michaud, N. Richarad, G. Ross, A. Sarkissian, B. L. Standsfield, B. Terreault, and W. Zuzak, Phys. Plasmas **1**, 1497 (1994).
[15] T. N. Todd and the COMPASS Team, Plasma Phys. Controlled Fusion **35**, B231 (1992).
[16] The Joint European Torus Team, Nucl. Fusion **32**, 187 (1992).